Phys. Med. Biol. **44** (1999) 323–333. Printed in the UK PII: S0031-9155(99)98086-7

Clinical relative biological effectiveness of low-energy x-rays emitted by miniature x-ray devices

David J Brenner†‡, Cheng-Shiun Leu†, John F Beatty§ and Ruth E Shefer‖

† Center for Radiological Research, Columbia University, 630 West 168th Street, New York, NY 10032, USA

§ Radiation Oncology Department, Massachusetts General Hospital, Boston, MA 02114, USA

‖ Newton Scientific Inc., Cambridge, MA 02141, USA

Received 5 October 1998

Abstract. Several groups are developing ultra-miniature x-ray machines for clinical use in radiation therapy. Current systems are for interstitial radiosurgery and for intravascular insertion for irradiation to prevent re-stenosis. Typical generating voltages are low, in the 20 to 40 kV range. It is well established that the biological effectiveness of such low-energy photons is large compared with higher-energy gamma rays, because of the dominance of photoelectric absorption at low energies. We have used microdosimetric analyses to estimate RBEs for such devices, both at low doses and clinically relevant doses, relative to radiations from ^{60}Co, ^{192}Ir, ^{125}I and ^{90}Sr/^{90}Y. The RBEs at clinically relevant doses and dose rates for these low-energy x-ray sources are considerably above unity, both relative to ^{60}Co and to ^{192}Ir photons, and also relative to ^{125}I and ^{90}Sr/^{90}Y brachytherapy sources. As a function of depth, the overall effect of the change in dose and the change in beam spectrum results in beams whose biologically weighted dose (dose × RBE) decreases with depth somewhat more slowly than does the physical dose. The estimated clinically relevant RBEs are sufficiently large that they should be taken into account during the treatment design stage.

1. Introduction

Several groups are developing ultra-miniature x-ray machines for clinical use in radiation therapy. One system (Dinsmore *et al* 1996), currently undergoing clinical trial (Cosgrove *et al* 1997, Kubo *et al* 1998) for interstitial radiosurgery, transports electrons along a long thin target tube which can be inserted along the track left by a biopsy cannula, such that the x-ray production target is adjacent to or inside a brain tumour. A different approach (Shefer *et al* 1998, Chornenky 1998) involves miniaturizing the entire x-ray generating device, which can then be inserted intravascularly, with the aim of allowing local irradiation after coronary angioplasty, to prevent or delay re-stenosis.

Both types of devices involve low x-ray generating voltages, both out of practicality and to optimize dose distributions over the target region. Typical generating voltages are 40 kV for the interstitial radiosurgery system and 20 kV for the intravascular device.

It is, however, now well established that the relative biological effectiveness (RBE) of photons increases with decreasing photon energy (ICRU 1986, Brenner and Amols 1989). This observation is both well established experimentally and well understood mechanistically. The phenomenon is understood theoretically, in that as the energy of the photons decreases, the energy of the secondary electrons emitted in the photon interactions decreases, with a

‡ E-mail address: djb3@columbia.edu

0031-9155/99/020323+11$19.50

corresponding increase in stopping power (linear energy transfer, LET). For example, the LET of a 15 keV secondary photoelectron is around 2 keV μm^{-1}, which is about an order of magnitude greater than the LET of a 500 keV electron.

That low-energy x-rays (with mean energies in the range from, say, 4 to 40 keV) have an increased biological effectiveness has been demonstrated in a variety of different biological systems, for example by Virsik *et al* (1977) and Sasaki *et al* (1989) for chromosome aberrations in human lymphocytes, by Verhaegen and Vral (1994) for micronuclei in human lymphocytes, by Zeitz *et al* (1977) and Marchese *et al* (1990) for clonogenic survival in cells of human origin, by Arslan *et al* (1986) for cell survival and chromosome aberrations in rodent cells, and by Bistrovic *et al* (1986), Hoshi *et al* (1988), Spadinger and Palcic (1992) and Ling *et al* (1995) for cell survival in rodent cells.

In the following, based on measured or calculated photon energy spectra from these miniature x-ray machines, we calculate RBEs firstly at low doses and then at clinically relevant doses.

2. Materials and methods

2.1. Relative biological effectiveness at low doses

The large differences in energy deposition patterns which underlie the differences in RBE with changing photon energy can by quantified through energy deposition spectra in micrometre sized targets, as shown in figure 1. Specifically, the energy deposition pattern in individual cells can be quantified (ICRU 1983) in terms of the distribution of lineal energy (y, the microdosimetric correlate of LET), defined as the energy deposited (by, in this case, an incident photon) in a given target size divided by the mean path length of the target.

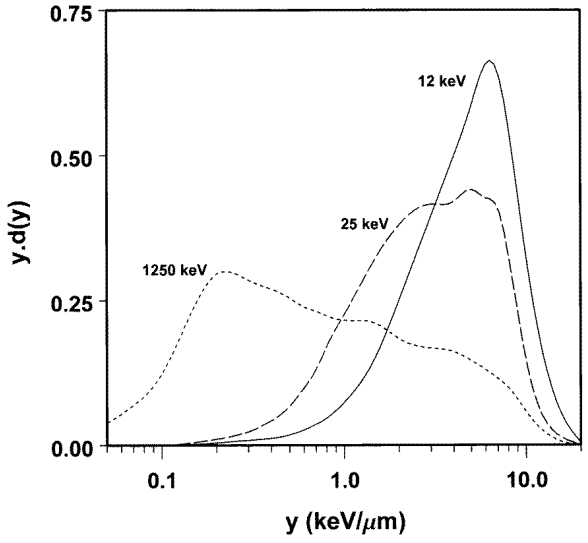

Figure 1. Measured microdosimetric energy deposition spectra in 1 μm site sizes, for various monoenergetic photons (after Kliauga and Dvorak 1978). The representation is such that the area under the curves delimited by any lineal energy (y) values is proportional to the fraction of dose deposited by photons in that energy range. As the photon energy increases, there is a significant shift in the energy deposition pattern towards lower lineal energy (y) values.

At low doses, the energy deposition patterns, $d(y)$, in individual cells or substructures of cells must determine the relative biological effect of one radiation to another. In such a situation, all that changes, for a given dose, from radiation to radiation, is the distribution of energy deposited in target cells—which is exactly the information in a microdosimetric spectrum. For a given low dose, the response, α (per unit dose), of a biological endpoint, ε, to a given radiation quality, i, can be written (Zaider and Brenner 1985)

$$\alpha_{\varepsilon i} = \int w_\varepsilon(y)\, d_i(y)\, \mathrm{d}y \tag{1}$$

where $d_i(y)$ is the normalized distribution of dose in lineal energy for radiation type i (see figure 1), and $w_\varepsilon(y)$ is the relative effect for endpoint ε as a function of lineal energy. In other words, cells respond with a biological response function (or weighting factor) $w_\varepsilon(y)$ (independent of the radiation, but characteristic of the endpoint) to a range of energy depositions $d_i(y)$ (independent of the endpoint but characteristic of the radiation), producing a total response $\alpha_{\varepsilon i}$. Equation (1) is valid for predicting relative biological effects at low doses even if the mechanism of cellular inactivation involves interaction between autonomous cells, or promoting factors, as long as these processes are independent of radiation quality.

The first quantitative estimates of the biological response function $w_\varepsilon(y)$ were for the endpoint of chromosomal aberrations in human lymphocytes (Zaider and Brenner 1985), and the function has also been extracted for the endpoint of HPRT mutation in human fibroblasts (Zaider and Brenner 1986), oncogenic transformation in rodent cells (Brenner *et al* 1995) and for cellular inactivation endpoints (Varma and Zaider 1992).

We estimated microdosimetric spectra, $d(y)$, corresponding to the low-energy photons emitted by the two miniature x-ray devices, as a function of distance from the source. These were then folded (see equation (1)) with a relevant biological response function $w_\varepsilon(y)$ to obtain estimates of the relative low-dose effectiveness of these x-rays.

The energy deposition spectrum, $d(y)$ for these different photon fields was calculated based on spectra for monoenergetic photons, using the following relation (Goodhead and Brenner 1983)

$$d(y) = \int E\, N(E)\, d(y;\, E) \mu_{\mathrm{en}}(E)/\rho\, \mathrm{d}E \tag{2}$$

where $N(E)$ is the fluence of photons at energy E, and $\mu_{\mathrm{en}}(E)/\rho$ is the mass-energy absorption coefficient in ICRU-44 average soft tissue (adult male; ICRU 1992) of density ρ, at photon energy E. $d(y;\, E)$ is the normalized spectrum of lineal-energy depositions for monoenergetic photons of energy E; above 12 keV, these spectra for monoenergetic photons were taken from measurements (Kliauga and Dvorak 1978; see figure 1) in a 1 μm equivalent-diameter wall-less proportional counter, which include data for 11.9, 25, 36, 60, 140, 320, 662 and 1250 keV photons. Between 3 and 12 keV, microdosimetric spectra were calculated assuming only photoelectric photon interactions, using the track structure simulation techniques described by Zaider and colleagues (Zaider *et al* 1983, Brenner and Zaider 1984), together with an energy resolution normalized to reproduce the experimental data (Kliauga and Dvorak 1978) at 11.9 keV. Interpolation of the measured microdosimetric spectra between photon energies was achieved using a two-dimensional interpolation scheme described by Akima (1978).

As we discuss below, we have also calculated a microdosimetric spectrum for a beta emitter, ^{90}Sr (in equilibrium with ^{90}Y). Analogously to equation (2), the microdosimetric spectrum was calculated by combining corresponding spectra for monoenergetic electrons of energy E_e:

$$d(y) = \int N(E_e)\, d(y;\, E_e) S(E_e)\, \mathrm{d}E_e \tag{3}$$

where $N(E_e)$ is the fluence spectrum of the beta source (taken, for an encapsulated $^{90}Sr/^{90}Y$ source, from the measurements of Faw *et al* (1990)) and $S(E_e)$ is the electron stopping power in ICRU-44 average soft tissue (adult male; ICRU 1992). $d(y; E_e)$ are the microdosimetric spectra for monoenergetic electrons of energy E_e, which were calculated using the DELTA Monte Carlo electron–proton transport code (Zaider *et al* 1983), using techniques described by Brenner and Zaider (1984) and Wuu *et al* (1996). Apart from the effect of the source encapsulation, no account was taken of electron scattering on the electron fluence spectrum.

2.2. Relative biological effectiveness at clinically relevant doses

In order to estimate RBEs at higher doses, we need a model describing dose-effect relationships. In the following we use the linear-quadratic (LQ) formalism, which is now almost universally used for clinical applications. The LQ formalism describes a biophysical model of cell killing, and its clinical application has been extensively discussed in the literature (Fowler 1989, Brenner *et al* 1998, Rossi and Zaider 1996, Thames and Hendry 1987).

In the LQ formalism, the yield (Y) of lethal lesions for a dose D of radiation type i, and the corresponding survival (S) equation are

$$Y_i \propto \alpha_i D_i + G\beta D_i^2 \qquad S_i = \exp(-Y_i) \tag{4}$$

where α and β are model parameters (α depending on the endpoint and the radiation type, while β depends on the biological endpoint only). G is the generalized Lea–Catcheside time factor, which accounts quantitatively for dose protraction (Brenner *et al* 1998); for continuous irradiation at a constant dose-rate for time T, this factor is

$$G = [2/(\lambda T)^2](\theta - 1 + \lambda T) \tag{5}$$

where $\theta = \exp(-\lambda T)$ and $\lambda = \ln(2)/T_{1/2}$, where $T_{1/2}$ is the half-time for sublethal damage repair. For $T \ll T_{1/2}$, $G = 1$.

In fact, equation (4) follows from the assumption that the biological response function $w(y)$ increases linearly with lineal energy, y (Rossi and Zaider 1996), which is a reasonable approximation at lineal energies less than about 100 keV μm^{-1} (i.e. for all the radiations of interest here, as shown in figure 1).

Equality of the observed effect for two types of radiation $i = H$ and $i = L$ (the notation refers to radiations of high and low biological effectiveness), delivered over the same time, implies

$$\zeta_H D_H + G D_H^2 = \zeta_L D_L + G D_L^2 \tag{6}$$

where $\zeta_i = \alpha_i/\beta$. Thus the RBE, D_L/D_H, of radiation H relative to radiation L as a function of dose D_H, is given by

$$\mathrm{RBE}(D_H) = \frac{\zeta_L}{2GD_H}\left[\sqrt{1 + \frac{4G}{\zeta_L}\left(\frac{\alpha_H}{\alpha_L}D_H + \frac{G}{\zeta_L}D_H^2\right)} - 1\right] \tag{7}$$

where α_H/α_L is the quantity which can be calculated from microdosimetric arguments (equation (1), see above). The ratio ζ_L, i.e. the α/β ratio for the reference radiation, is a quantity that has been repeatedly evaluated (Fowler 1989, Brenner *et al* 1998, Rossi and Zaider 1996, Thames and Hendry 1987). For most tumours exposed to megavoltage photons, ζ_L is typically in the range from 7–10 Gy (Thames and Hendry 1987).

3. Results

3.1. X-ray fluence spectra

Figure 2 shows measured photon energy spectra (Beatty *et al* 1996) from the miniature photon radiosurgery system, operated at 40 kVp. Spectra are shown for various distances (in water) from the source, from 0 to 20 mm. Figure 3 shows comparable spectra as a function of depth, calculated using the TIGER electron–photon transport codes (Halbleib and Melhorn 1984) and the MCNP neutron/photon transport code (Briesmeister 1997), for a miniature source designed for intravascular insertion, operated at 20 kVp with a tungsten anode. In this latter case, depths of interest range from 0 to 3 mm.

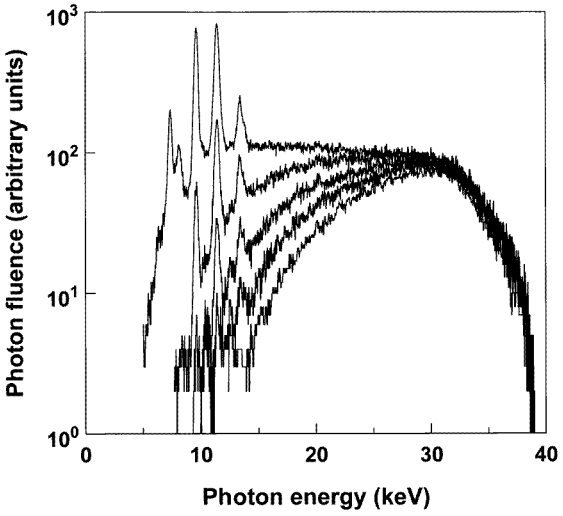

Figure 2. Measured photon fluences (after Beatty *et al* 1996) as a function of distance in water from the x-ray source of a miniature photon radiosurgery system (Dinsmore *et al* 1996, Cosgrove *et al* 1997). Top curve is in air; lower curves show spectra at 5 mm increments up to 20 mm.

As reference radiations, for both x-ray sources, we have considered ^{60}Co gamma rays (average energy 1252 keV) and ^{192}Ir gamma rays (average energy 375 keV). Over the depths of interest here ($<$20 mm), the changes in the energy spectra of these two reference radiations are negligible. In addition, because they represent different brachytherapy modalities that have been used clinically, we have also considered as reference radiations the gamma emitter ^{125}I (for the photon radiosurgery system, average energy after encapsulation $\sim$28 keV), and the beta emitter ^{90}Sr (for the vascular irradiation system, in equilibrium with ^{90}Y). The spectra for both these radiations will change with depth over the depths of interest here, and we have evaluated RBEs relative to these radiations only at zero depth.

3.2. Calculated low-dose relative biological effectiveness

Of the various biological endpoints, ε, for which biological response weighting functions $w_\varepsilon(y)$ (see equation (1)) have been evaluated, we have chosen to use that of dicentric chromosomal aberration formation in human lymphocytes (Zaider and Brenner 1985). Our rationale is that cell killing at clinical doses is directly correlated with the yield of dicentric aberrations (Wlodek

and Hittelman 1988), and this particular $w_\varepsilon(y)$ function is the most extensively characterized in all relevant regions of y of any such evaluated function (ICRU 1986).

Table 1 shows the predicted low-dose RBEs (α_H/α_L) for the photon radiosurgery system, operated at 40 kV. The results are tabulated relative to those of gamma rays from ^{60}Co and ^{192}Ir. Comparable results are shown in table 2 for the miniature vascular irradiator, operated at 20 kV. As expected, the RBE's for the lower-energy vascular irradiator are somewhat higher than for the 40 kV radiosurgical device. The photon spectra harden somewhat as a function of depth, resulting in a decrease in low-dose RBE.

Table 1. Estimated low-dose RBEs (α_H/α_L; see equation (1)) and clinically relevant RBEs (23 min irradiation, 12.5 Gy) for low-energy x-rays as shown in figure 2, for a miniature photon radiosurgery system (Dinsmore *et al* 1996, Cosgrove *et al* 1997), operated at 40 kV.

	versus ^{60}Co		versus ^{192}Ir		versus ^{125}I	
Depth (mm)	Low dose	Clinical	Low dose	Clinical	Low dose	Clinical
0	3.05	1.53	2.11	1.38	1.23	1.12
5	2.67	1.44	1.85	1.29		
10	2.54	1.41	1.76	1.27		
15	2.48	1.40	1.72	1.25		
20	2.44	1.40	1.69	1.24		

Table 2. Estimated low-dose RBEs (α_H/α_L; see equation (1)) and clinically relevant RBEs (15 min irradiation, 15 Gy) for low-energy x-rays as shown in figure 3, for a miniature vascular irradiator device (Shefer *et al* 1998, Chornenky 1998), operated at 20 kV.

	versus ^{60}Co		versus ^{192}Ir		versus ^{90}Sr/^{90}Y	
Depth (mm)	Low dose	Clinical	Low dose	Clinical	Low dose	Clinical
0	3.62	1.54	2.51	1.43	4.62	1.60
0.9	3.45	1.51	2.39	1.38		
1.4	3.26	1.48	2.26	1.35		
1.9	3.22	1.47	2.23	1.34		
2.4	3.20	1.47	2.22	1.34		
2.9	3.19	1.46	2.21	1.34		

3.3. Calculated relative biological effectiveness at clinically relevant doses

Based on the low-dose RBEs shown in tables 1 and 2, equation (7) can be used to estimate RBEs at clinical doses and dose rates. Apart from the quantity α_H/α_L, which is shown in tables 1 and 2, we also need the quantity ζ_L (i.e. the alpha/beta ratio for the reference radiation), and the quantity $T_{1/2}$ (see equation (5)), the half-time for sublethal damage repair.

For high-energy gamma rays, the quantity ζ_L (i.e. α_L/β) has been evaluated for many clinically relevant endpoints (Thames and Hendry 1987). For the early-responding endpoints of relevance to the current applications, α_L/β is typically of the order of 7–10 Gy for photons of energy 1 MeV and higher. In the calculations that follow, we have therefore used a value of 8 Gy for ^{60}Co gamma rays and, based on the calculated ratios (see tables 1 and 2) of low-dose RBEs relative to ^{60}Co, we have respectively used α_L/β values of 11.5, 19.8 and 6.3 Gy for the calculations involving reference radiations ^{192}Ir, ^{125}I and ^{90}Sr/^{90}Y.

In our calculations, we have used a typical value for $T_{1/2}$ of 15 min (Brenner and Hall 1991); the clinical RBEs are not very sensitive to the particular value of $T_{1/2}$ chosen (within

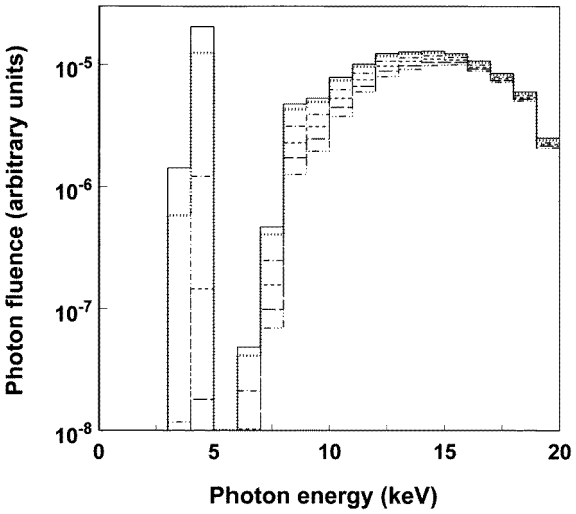

Figure 3. Calculated photon fluences as a function of distance in tissue from the x-ray source of a miniature vascular irradiator device (Shefer *et al* 1998). Top curve is immediately outside the titanium window; lower curves show spectra at distances of 0.9, 1.4, 1.9, 2.4 and 2.9 mm.

reasonable limits), reflecting the fact (see below) that the RBEs do not vary strongly with time over the range of irradiation times that might practically be used. Specifically, for the vascular irradiator, we have performed calculations for exposures of 1 and 15 min (the latter being a typical estimated exposure time), while for the radiosurgery irradiator, we have performed calculations for irradiation times of 7, 23 and 45 min, the range of irradiation times used in early clinical trials (Cosgrove *et al* 1997).

Typical results for clinical RBEs are shown in figures 4 and 5 and in tables 1 and 2. The photon radiosurgery system, operated at 40 kVp, has been used in the dose range from 10–15 Gy, with a mean dose of 12.5 Gy and a mean exposure time of 23 min (Cosgrove *et al* 1997). Under these average conditions: (a) the estimated RBE at this dose relative to ^{60}Co gamma rays varies from about 1.53 at the source, to about 1.40 at a depth of 20 mm; (b) relative to ^{192}Ir, this estimated RBE varies with depth from about 1.38 to 1.24; and (c) relative to ^{125}I photons, this RBE is estimated to be about 1.12 close to the source.

The vascular irradiator is likely to be used in the dose range from 10 to 25 Gy (Weinberger and Simon 1997, Brenner *et al* 1996). At a dose of 15 Gy and a projected irradiation time of 15 min, the RBE relative to ^{60}Co gamma rays is likely to be around 1.5, with comparatively little variation over a 2 mm depth; relative to ^{192}Ir, this estimated RBE is about 1.35, and relative to a ^{90}Sr/^{90}Y beta emitter, the estimated RBE near the source is 1.60. It should be noted that the estimated RBE relative to ^{90}Sr/^{90}Y may be a slight overestimate, as the effects of electron scattering (other than from the source encapsulation) were not taken into account.

It is important to note that the decrease in clinically relevant RBE with depth shown, for example, in tables 1 and 2, is *for a given dose*. For any given geometry, the dose decreases with depth, and the RBE increases with decreasing dose, so the actual RBEs generally *increase* with depth. For example, based on the depth-dose profile shown by Douglas *et al* (1996) for the photon radiosurgery system, a dose of 12.5 Gy at a treatment radius of 15 mm would decrease to 5.2 Gy at 20 mm; while the RBEs relative to ^{192}Ir *at 12.5 Gy* for 15 and 20 mm are respectively 1.25 and 1.24 (see table 1), a more useful comparison is between the RBE at 15 mm and 12.5 Gy (RBE $=$ 1.25) with the RBE at 20 mm and 5.2 Gy (RBE $=$ 1.38, see

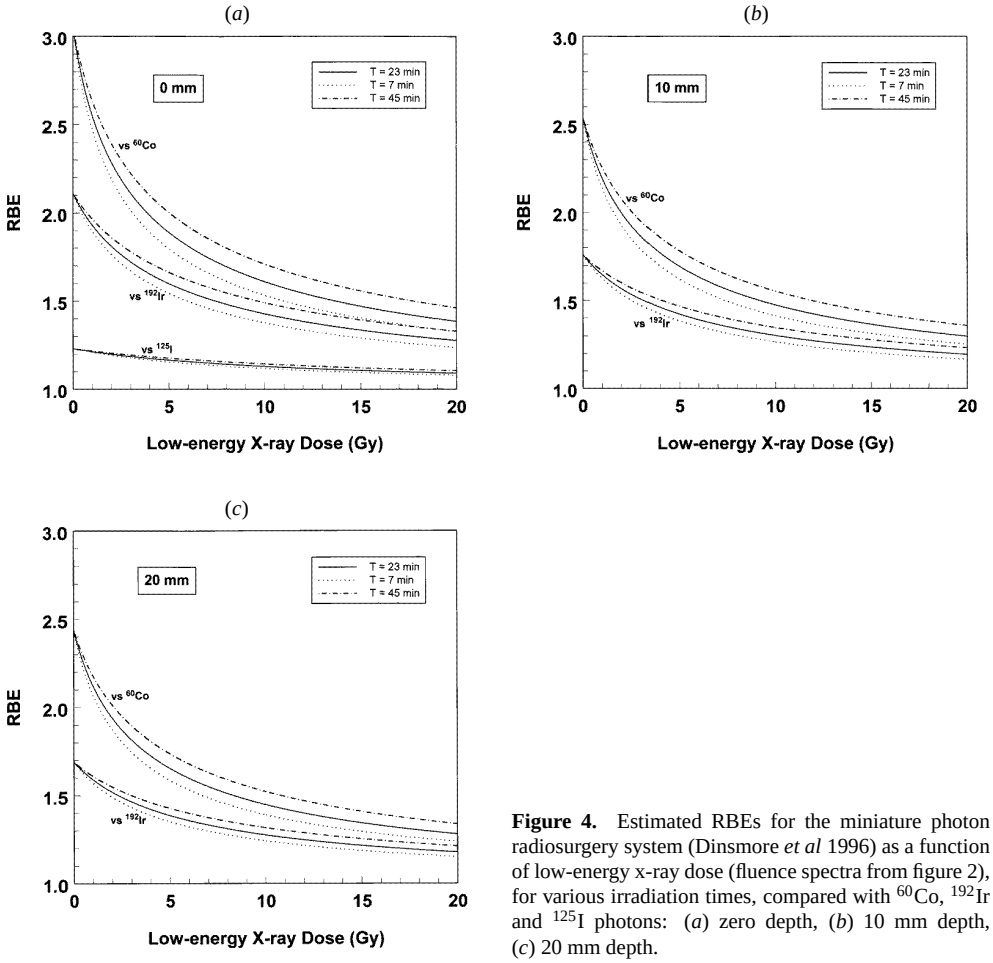

Figure 4. Estimated RBEs for the miniature photon radiosurgery system (Dinsmore *et al* 1996) as a function of low-energy x-ray dose (fluence spectra from figure 2), for various irradiation times, compared with ^{60}Co, ^{192}Ir and ^{125}I photons: (*a*) zero depth, (*b*) 10 mm depth, (*c*) 20 mm depth.

figure 4(*c*)). In other words the decrease in RBE with depth due to beam hardening is more than compensated for by the increase in RBE with depth due to the decreasing dose. The overall effect, both for the photon radiosurgical system and the vascular irradiator device, are beams whose fall-off of biologically weighted dose (dose $\times$ RBE appropriate for that dose) with depth is somewhat slower than the fall-off of physical dose with depth.

4. Discussion

Both from experimental results, and the current calculations, it is clear that the RBEs at clinically relevant doses and dose rates for these low-energy x-ray sources are considerably greater than unity, both relative to ^{60}Co and to ^{192}Ir photons, and also relative to ^{125}I and ^{90}Sr/^{90}Y brachytherapy sources. As a function of depth, the overall effect of the change in dose and the change in beam spectrum results in beams whose biologically weighted dose (dose $\times$ RBE) decreases with depth somewhat more slowly than does the physical dose.

The estimated clinically relevant RBEs are sufficiently large that they should be taken into account during the treatment design stage. Assuming this to be the case, the increased RBE

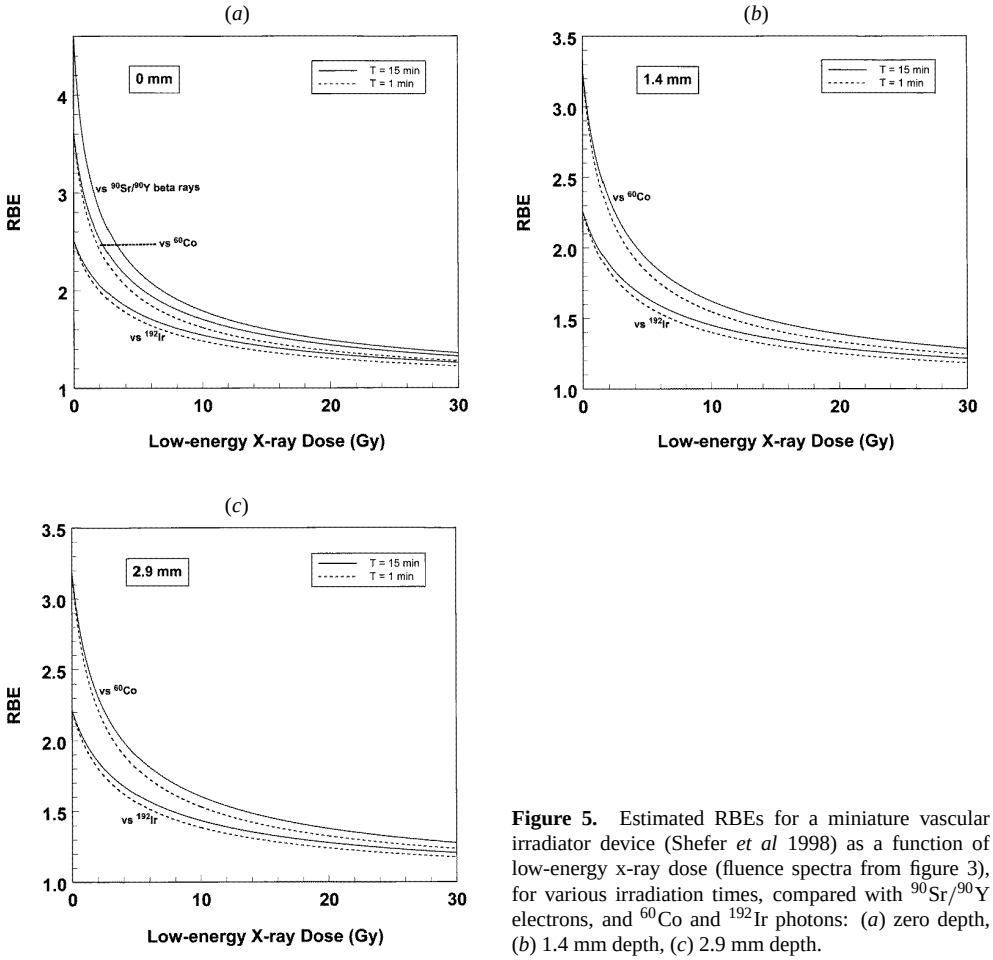

Figure 5. Estimated RBEs for a miniature vascular irradiator device (Shefer *et al* 1998) as a function of low-energy x-ray dose (fluence spectra from figure 3), for various irradiation times, compared with $^{90}Sr/^{90}Y$ electrons, and ^{60}Co and ^{192}Ir photons: (*a*) zero depth, (*b*) 1.4 mm depth, (*c*) 2.9 mm depth.

may be considered an advantage for these new miniature machines, in that it decreases the dose and thus the exposure time necessary to yield the same biological effect.

Finally it is important to recognize that the RBE values given here, though based on reasonable biological models, are nonetheless estimates, which should be used with caution in clinical situations.

Acknowledgments

This work was partially supported by NCI grants CA-24232, CA-49062, CA-77285 and DOE grant DE-FG02-98ER62686.

References

Akima H 1978 A method of bivariate interpolation and smooth surface fitting for irregularly distributed data points *ACM Trans. Math. Software* **4** 148–59

Arslan N C, Geard C R and Hall E J 1986 Low dose-rate effects of cesium-137 and iodine-125 on cell survival, cell progression and chromosome alterations *Am. J. Clin. Oncol.* **9** 521–6

Beatty J, Biggs P J, Gall K, Okunieff P, Pardo F S, Harte K J, Dalterio M J and Sliski A P 1996 A new miniature x-ray device for interstitial radiosurgery: dosimetry *Med. Phys.* **23** 53–62

Bistrovic M, Biscan M and Viculin T 1986 RBE of 20 kV and 70 kV x-rays determined for survival of V79 cells *Radiother. Oncol.* **7** 175–80

Brenner D J and Amols H I 1989 Enhanced risk from low-energy screen-film mammography x-rays *Br. J. Radiol.* **62** 910–14

Brenner D J and Hall E J 1991 Conditions for the equivalence of continuous to pulsed low dose rate brachytherapy *Int. J. Radiat. Oncol. Biol. Phys.* **20** 181–90

Brenner D J, Hlatky L R, Hahnfeldt P J, Huang Y and Sachs R K 1998 The linear-quadratic and most other common radiobiological models result in similar predictions of time-dose relationships *Radiat. Res.* **150** 83–91

Brenner D J, Miller R C and Hall E J 1996 The radiobiology of intravascular irradiation *Int. J. Radiat. Oncol. Biol. Phys.* **36** 805–10

Brenner D J, Miller R C, Huang Y and Hall E J 1995 The biological effectiveness of radon-progeny alpha particles; III Quality factors *Radiat. Res.* **142** 61–9

Brenner D J and M Zaider 1984 The application of track calculations to radiobiology—II: Calculations of microdosimetric quantities *Radiat. Res.* **98** 14–25

Briesmeister J F (ed) 1997 MCNP—a general Monte Carlo n-particle transport code *Los Alamos National Laboratory Report* LA-12625-M

Chornenky V I 1998 The soft x-ray system *Handbook of Vascular Brachytherapy* ed R Waksman and P W Serruys (London: Martin Dunitz)

Cosgrove C R, Hochberg F H, Zervas N T, Pardo F S, Valenzuela R F and Chapman P 1997 Interstitial irradiation of brain tumors, using a miniature radiosurgery device: initial experience *Neurosurgery* **40** 518–23

Dinsmore M, Harte K J, Sliski A P, Smith D O, Nomikos P M, Dalterio M J, Boom A J, Leonard W F, Oettinger P E and Yanch J C 1996 A new miniature x-ray source for interstitial radiosurgery: device description *Med. Phys.* **23** 45–52

Douglas R M, Beatty J F, Gall K, Valenzuela R F, Biggs P, Okunieff P and Pardo F S 1996 Dosimetric results from a feasibility study of a novel radiosurgical source for irradiation of intracranial metastases *Int. J. Radiat. Oncol. Biol. Phys.* **36** 443–50

Faw R E, Simons G G, Gianakon T A and Bayouth J E 1990 Simulation of angular and energy distributions of the PTB beta secondary standard *Health Phys.* **59** 311–24

Fowler J F 1989 The linear-quadratic formula and progress in fractionated radiotherapy *Br. J. Radiol.* **62** 679–94

Goodhead D T and Brenner D J 1983 Estimation of a single property of low-LET radiations which correlates with biological effectiveness *Phys. Med. Biol.* **28** 485–92

Halbleib J A and Melhorn T A 1984 ITS: the integrated TIGER series of coupled electron/photon Monte-Carlo transport codes *Sandia National Laboratory Report* SAND 84-0573

Hoshi M, Antoku S, Nakamura N, Russell W J, Miller R C, Sawada S, Mizuno M and Nishio S 1988 Soft x-ray dosimetry and RBE for survival of Chinese hamster V79 cells *Int. J. Radiat. Biol.* **54** 577–91

ICRU 1983 Microdosimetry *ICRU Report* 36 (Bethesda, MA: International Commission on Radiation Units and Measurements)

——1986 The quality factor in radiation protection *ICRU Report* 40 (Bethesda, MA: International Commission on Radiation Units and Measurements)

——1992 Photon, electron, proton and neutron interactions in tissue *ICRU Report* 46 (Bethesda, MA: International Commission on Radiation Units and Measurements)

Kliauga P and Dvorak R 1978 Microdosimetric measurements of ionization by monoenergetic photons *Radiat. Res.* **73** 1–20

Kubo O, Muragaki Y, Iseki H and Takakura K 1998 Clinical evaluation of intraoperative radiotherapy using radiosurgery system of brain tumors *Gan-to Kagaku Ryōhō* **25** 1348–51

Ling C C, Li W X and Anderson L L 1995 The relative biological effectiveness of I-125 and Pd-103 *Int. J. Radiat. Oncol. Biol. Phys.* **32** 373–8

Marchese M J, Goldhagen P E, Zaider M, Brenner D J and Hall E J 1990 The relative biological effectiveness of photon radiation from encapsulated I-125, assessed in cells of human origin *Int. J. Radiat. Oncol. Biol. Phys.* **18** 1407–13

Rossi H H and Zaider M 1996 *Microdosimetry and its Applications* (Berlin: Springer)

Sasaki M S, Kobayashi K, Hieda K, Yamada Y, Ejima Y, Maezawa H, Furusawa Y, Ito T and Okada S 1989 Induction of chromosome aberrations in human lymphocytes by monochromatic x-rays of quantum energy between 4.8 and 14.6 keV *Int. J. Radiat. Biol.* **56** 975–88

Shefer R E, Hughey B J, Klinkowstein R E and Brenner D J 1998 Dosimetry of intravascular soft x-ray sources for restenosis therapy *Advances in Cardiovascular Radiation Therapy II (Washington, DC, 8–10 March 1998)* (Washington, DC: Cardiology Research Foundation, Washington Hospital Center and Washington Cancer Institute) p 13

Spadinger I and Palcic B 1992 The relative biological effectiveness of ^{60}Co gamma-rays, 55 kVp x-rays, 250 kVp x-rays, and 11 MeV electrons at low doses *Int. J. Radiat. Biol.* **61** 345–53

Thames H D and Hendry J H 1987 *Fractionation in Radiotherapy* (New York: Taylor and Francis)

Varma M N and Zaider M 1992 A non-parametric, microdosimetric-based approach to the evaluation of the biological effects of low doses of ionizing radiation *Biophysical Modelling of Radiation Effects* ed K H Chadwick, G Moschini and M N Varma (Bristol: Adam Hilger) pp 145–53

Verhaegen F and Vral A 1994 Sensitivity of micronucleus induction in human lymphocytes to low-LET radiation qualities: RBE and correlation of RBE and LET *Radiat. Res.* **139** 208–13

Virsik R P, Harder D and Hansmann I 1977 The RBE of 30 kV x-rays for the induction of dicentric chromosomes in human lymphocytes *Radiat. Environ. Biophys.* **14** 109–21

Weinberger J and Simon A D 1997 Intracoronary irradiation for the prevention of restenosis *Curr. Opin. Cardiol.* **12** 468–74

Wlodek D and Hittelman W N 1988 The relationship of DNA and chromosome damage to survival of synchronized x-irradiated L5178Y cells—II: Repair *Radiat. Res.* **115** 566–75

Wuu C S, Kliauga P, Zaider M and Amols H I 1996 Microdosimetric evaluation of relative biological effectiveness for 103Pd, 125I, 241Am, and 192Ir brachytherapy sources *Int. J. Radiat. Oncol. Biol. Phys.* **36** 689–97

Zaider M and Brenner D J 1985 On the microdosimetric definition of quality factors *Radiat. Res.* **103** 302–16

——1986 Evaluation of a specific quality function for mutation induction in human fibroblasts *Radiat. Prot. Dosim.* **15** 79–82

Zaider M, Brenner D J and Wilson W E 1983 The application of track calculations to radiobiology—I: Monte Carlo simulation of proton tracks *Radiat. Res.* **95** 231–47

Zeitz L, Kim S H, Kim J H and Detko J F 1977 Determination of relative biological effectiveness (RBE) of soft x-rays *Radiat. Res.* **70** 552–63